Assessment of SAMPSON Severe Accident Code Modeling against MAAP-MELCOR Crosswalk

Ayumi Itoh, Marco Pellegrini, Masanori Naitoh
The Institute of Applied Energy
1-14-2 Nishi-Shimbashi, Minato-ku, Tokyo, Japan
a-ito@iae.or.jp, mpellegrini@iae.or.jp, mnaito@iae.or.jp

ABSTRACT
Analytical investigation by computational simulation is expected to provide essential information such as the ex-vessel status of the core debris. Severe accident analysis codes, however, can present different predictions depending on the modeling assumptions. Therefore understanding how the modeling affects the result of the simulations is important. In this study, SAMPSON simulations are compared against MAAP-MELCOR crosswalk results [1] with the specific assumptions provided for core inventory and water inventory and accident scenarios for Fukushima Daiichi NPP UN-1. The key phenomena characterizing core damage progression are core oxidation, core melting, debris relocation, corium debris slumping into the lower plenum and lost of the RPV integrity. There are some discrepancies about hydrogen production and water level transient. SAMPSON shows rapid and large amount of hydrogen generation and the water level decreases quickly. These discrepancies are thought to come from the oxidation model differences between two codes. In this paper, main key parameters are compared and the discrepancies observed are investigated.

KEYWORDS
SAMPSON, MELCOR, MAAP, Fukushima, Unit 1

1. INTRODUCTION

The Fukushima Daiichi nuclear power station accident occurred in March 2011. All units are believed to experience severe accident involving core melting due to the loss of cooling capability. An enormous effort has been done for understanding the accident progression using various different Severe Accident (SA) computer codes. Because each analysis employs different plant nodalizations and boundary conditions, every analysis predicts unique accident progressions with varing degrees of agreement with data. As it has been shown in the project “Benchmark Study of the Accident at the Fukushima Daiichi nuclear power station (BSAF)” conducted by the OECD/NEA [2], that also using the same boundary and initial conditions as common case. Therefore, it is important to understand how different model assumptions affect the simulation results and further analyses are required to gain a better understanding of the Fukushima accidents. A study on the impact of the different modelling on the results has been done with MAAP5 and MELCOR [3] as reported in the MAAP-MELCOR Crosswalk [1]. In the crosswalk study, the simulation of the Fukushima Daiichi Unit 1 accident under exact same boundary conditions and assessed against in-vessel core melt progression from onset of core damage to breach of the RPV lower head was performed. We concentrated on the comparison of SAMPSON with MELCOR as the first attempt of this study because there published enormous analysis results or information about MELCOR. The main objective of this paper is to clarify the significant modeling assumptions which cause different simulation results obtained using the SAMPSON and the MELCOR code.

2. FUKUSHIMA DAIICHI ACCIDENT PROGRESSION OF UNIT 1

The Great East Japan earthquake occurred on March 11th 2011 at 14:46, which was followed by a tsunami which is estimated to have reached the height of 14 m and hit the Fukushima Daiichi nuclear power station. In the Unit 1, the shutdown of the reactor was accomplished and for the first hour before the arrival of the tsunami, the isolation condensers (IC) were activated by closure of the main

steam isolation valve (MSIV). However, the IC operation was shut down manually before the arrival of tsunami and all AC and DC power was lost, which resulted in the lost of cooling capability to cause the increases of the temperature and pressure of the reactor until alternative water injection started at 13 hours later the SCRAM. It is still uncertain to what extent this water injection worked for preventing accident progression. This study focuses on the early phase before the water injection which is considered that the core degradation had been progressed.

3. MAAP-MELCOR CROSSWALK

The MAAP-MELCOR Crosswalk was the study to develop the insights what causes the differences between two codes jointly sponsored by the Department of Energy: Office of Nuclear Energy (DOE-NE, United States) and the Electric Power Research Institute (EPRI, United States). Both MAAP and MELCOR simulation provide the information about the in-vessel accident analysis for understanding of the ex-vessel core debris status, however, it was realized that there was significant differences between two codes in the core melt discharge transient from the RPV lower head, which motivates their crosswalk study.
The following are the most significant differences between MAAP and MELCOR [1]:

- ✓ RPV pressure at time of RPV lower head breach;
- ✓ The fraction and temperature of molten material relocating into containment;
- ✓ The rate of core debris relocation into containment;
- ✓ The hydrogen generation transient and amount.

The parameters about in-vessel core melt progression from core oxidation onset to debris relocation into containment and the RPV thermal hydraulic response are compared with related model differences. It is realized that the most significant difference comes from the different manner to treat heat transfer from particulate debris to RPV fluid, which causes the difference in the hydrogen generation transient in the both code simulations.

4. SAMPSON CODE MODEL

SAMPSON is a code set for whole plant analysis under severe accident developed by the Nuclear Power Engineering Corporation (NUPEC, Japan) in the 1990s, which is composed of a number of independent modules representing physical phenomena and analysis. Overall plant response is calculated by these modules along with an accident progression. In this study, the code version SAMPSON-1.4.4 is used and model description is focused on the core degradation.

4.1. Core Degradation Model

The SAMPSON code models the core degradation by treating partial differential equations regarding the conservation laws for mass, momentum and energy in each core node. Once the fuel melting starts, interaction of molten materials with vessel atmosphere and peripheral structures is considered. The mass and energy conservation equations are solved in the phase change of melting of freezing processes. The mass and energy transferred from contacting other components with different phases through the interfacial areas are taken into account for solving the equations. The SAMPSON code assumes that heat sources are the decay heat from the fuel, and the chemical heat from the oxidation reactions.
Core degradation model in SAMPSON is composed of the following mechanisms:

- ✓ Fuel melting and relocation
- ✓ Fuel cladding rupture
- ✓ Control blade and fuel canister failure
- ✓ Lower core structure failure

4.1.1. Fuel Melting and Relocation

The Zircaloy cladding melt can start just above 2000 K, which causes dissolution of UO_2 pellet by molten Zircaloy. This interaction promotes the eutectic reaction between UO_2 and Zircaloy around

2300 K which is about 1000 K below their melting point. But relocation of the molten Zircaloy cladding may be delayed or prevented by protective ZrO_2 layer. SAMPSON assumes that they slump at 2473 K, which is the melting point of ZrO_2, with a fixed fraction of the dissolution of 0.2 kg UO_2 in 1 kg of molten Zircaloy. As the fuel temperature increases, UO_2 melts at its melting point of 3113 K.

4.1.2. Fuel Cladding Rupture

Oxidation of the Zircaloy cladding with steam created a ZrO_2 layer in the external of the cladding surface. The integrity of the cladding depends on the extent of the Zircaloy oxidation and temperature. SAMPSON calculates mechanical integrity and embrittlement of the cladding accounting for thickness of ZrO_2 layer, temperature and mechanical properties of material such as elastic or thermal expansion.

4.1.3. Control Blade and Fuel Canister Failure

Degradation of the control blade or fuel canister depend on chemical interactions among Zircaloy, stainless steel and B_4C. The B_4C control blade is composed of B_4C pellets clad in stainless steel. When the control blade heats up to 1500 K, the eutectic reaction between B_4C and stainless steel can begin. Additionally, the stainless steel in the control blade can interact with the Zircaloy on the fuel canister wall. These interactions result in early liquefaction of control blades and fuel canisters below their melting point, which are 1700 K for stainless steel and 2125 K for Zircaloy. SAMPSON treats the above model [4] but it is not employed in the present analysis.

4.1.4. Lower Core Structure Failure

Lower core structures such as core plate are assumed to melt at the melting point of stainless steel. Once they start melting and lose integrity to support the core, molten debris immediately starts falling into the lower plenum through rupture points. SAMPSON assumes that liquid components above the lower structure go to the lower plenum via failure nodes as continuous flow.

4.2. Oxidation Model

SAMPSON treats oxidation of the Zircaloy in the fuel cladding and fuel canister, the stainless steel in control blade. Metal materials in the debris can also be taken account for oxidation. The reaction rate of oxidation is determined accounting for the following factors.

- ✓ Availability of Zr or stainless steel;
- ✓ Availability of steam, which is determined by steam mass flow rate onto the surface;
- ✓ Steam diffusion on the structure surface of which steam moves to the lesser concentration area.

The correlation used for Zr oxidation are as follows.

- ✓ Below 1783 K, the Cathcart parabolic reaction kinetics correlation is applied;
- ✓ Above 1783 K, the Prater parabolic reaction kinetics correlation is applied.

Stainless steel oxidation is based on the parabolic oxidation constant model based on the MATPRO Version 11 Revision 2 [6]. SAMPSON uses the heat transfer area of the node as the oxidation surface area. SAMPSON does not assume that the solid debris bed completely block the flow and assumes that the node porosity cannot decrease below a minimum porosity for calculation stability.

4.3. Material Components

SAMPSON represents the degraded core in terms of composition of multi-phase component in the core node. Each node can be composed of nine liquid components, four solid structure components and six gas components and has their composition ratio. Liquid components except water can become particle component due to their temperature decreases in contact with water or steam. Particle components are assumed to be in the liquid phase since they are taken as continuous phase due to convection. The material groups considered by SAMPSON are shown in Table 1. Rod structure represents the fuel rod or control rod. Liquid and crust structure represents debris which is a mixture metal and its oxide.

Table 1. Material Components in SAMPSON

Phase	Component	Representing Materials
Liquid (Particle)	Water	H_2O
	Fuel	UO_2/U_3O_8
	Cladding	Zr/ZrO_2
	Control rod	B_4C
Structure	Rod	UO_2/U_3O_8 or B_4C
	Cladding	Zr/ZrO_2
	Internals	Fe/Fe_3O_4
	Crust	$Zr/ZrO_2/Fe/Fe_3O_4$
Gas	Steam	H_2O
	N_2, O_2, H_2, Ar, He	

4.4 Nodalisation

Heat-up of fuel rods and control rod until failure of fuel rods is evaluated with the two-dimensional axisymmetrical (R-Z coordinates) heat conduction model in the nodalisation of Fig. 1. Each rod represents a lamped number of assemblies in the active region and the rodhas 3 points in the radial direction plus 1 for the cladding and 10 in the axial direciton. The core region is composed of the active region and the lower core structure, which is divided into 8 channels each subdivided into 13 axial nodes. The lowest 3 axial region represents the lower core structure. The channel 1, 3, 5 and 7 represent the fuel channels composed of the fuel rod and fuel canister and the channel 2, 4 and 8 represent the bypass channels composed of the control rod and blade or shroud. Material component and its ratio in each node is employed as shown in Fig. 2. (ex. 45 % Steel structure is employed as the lower structure at channel 1 of height 3.) The structure component can melt and change its phase.

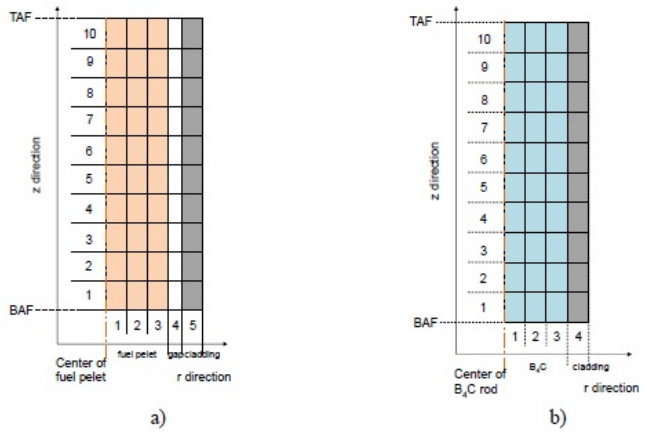

Fig. 1 SAMPSON Fuel Region Nodalisation for Fuel Rod Heat-up Analysis for a) fuel rod and b) control rod.

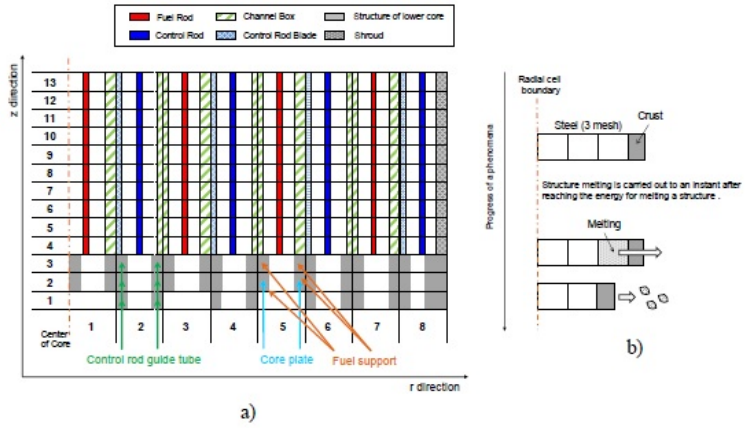

Fig. 2 SAMPSON Core Region Nodalisation for Molten Core Relocation Analysis for a) core region and b) structure.

5. ACCIDENT PROGRESSION ANALYSIS

The calculation for 9 hours after SCRAM was performed with SAMPSON 1.4.4. The same boundary conditions with the initial inventories of the core material in Table 2 and water in RPV in Table 3 were used. The following are event scenarios used in the calculation which are exact same as the MAAP-MELCOR crosswalk study [1]:

- ✓ MSIV (Main Steam Isolation Valve) closure signal at 52.5 seconds after SCRAM;
- ✓ The feedwater system is assumed to inject for the first 60 seconds after SCRAM;
- ✓ The period of IC (Isolation Condenser) operation is assumed as Table 4;
- ✓ SRV seizure at 7 hours after SCRAM;
- ✓ All discharge through the seized SRV is assumed to go into the suppression pool.
- ✓ The same decay heat curve is used for both the SAMPSON and MELCOR simulations.

Table 2. Initial inventory of the core material [kg]

Parameter	SAMPSON	MELCOR [3]
Number of fuel assemblies	400	400
Number of control blades	97	97
Mass of UO_2	77,867	77,200
Mass of B_4C	540	540
Mass of Zircaloy	28,288	28,250
Mass of stainless steel	17,834	17,880

Table 3. Initial inventory of water in RPV [kg]

Parameter	SAMPSON	MELCOR [3]
Core region	21,356	13,322
Downcomer	47,975	57,865
Jet pumps	3,512	3,015
Recirculation system	15,655	18,121
Lower plenum	38,350	39,127
Total	120,402	131,270

Table 4. IC Operation Period

Time of IC Operation Starts [s]	Time of IC Operation Ceases [s]	Number of IC Trains Operated
360	1020	2
1860	1980	1
2280	2400	1
2760	2880	1

The key event timings computed by SAMPSON under the above conditions are compared with those of MELCOR as shown in Table 4. The remarkable differences are water level decreasing rate and fuel assembly collapse timing. Since how quickly water boils away is determined by the amount of heat transferred to water, modelling difference of the way to treat heat from debris might cause these deviations. Considering both SAMPSON and MELCOR using the same decay heat curve, oxidation modelling difference is another key point. Although the parabolic kinetic correlation in the two codes are different, SAMPSON and MELCOR adopts similar philosophy for oxidation model [1]. Therefore, the differences in the factors participating on the oxidation such as the oxidation surface area and minimum porosity might be considered to cause these significant differences.

Table 5. Key event timings

Accident progression event	SAMPSON	MELCOR [3]
Time of complete MSIV closure	55.5s	55.5s
Time of loss of feedwater	60.0s	60.0s
Core swollen water level at TAF	2.9h	2.7h
Core swollen water level at BAF	3.9h	4.5h
Downcomer swollen water level at TAF	3.4h	2.6h
Downcomer swollen water level at BAF	4.7h	5.4h
Lower plenum dryout	5.60h	10.36h
Onset of hydrogen generation	3.8h	3.6h
Initial fuel assembly collapse Ring 1 (CH1)	3.9h	5.0h
Initial fuel assembly collapse Ring 2 (CH3)	4.1h	8.4h
Initial fuel assembly collapse Ring 3 (CH5)	4.1h	9.0h
Initial fuel assembly collapse Ring 4 (CH7)	4.1hs	no collapse
Initial fuel assembly collapse Ring 5	-	no collapse
Shroud failure	4.6h	event not predicted

5.1 RPV Response

5.1.1. RPV Pressure

The RPV pressure comparison is shown in Fig. 3. During the first hour after SCRAM, the RPV pressure is controlled by the IC operations. After the first hour, the RPV pressure increases up to the SRV activation point and the pressure is controlled by the SRV cycling. Until 7 hours at which the SRV seizure occurs, the calculation results are similar. Beyond 7 hours, both SAMPSON and MELCOR simulate RPV depressurization caused by the SRV seizure. The SAMPSON code predicts a quasi instaneous RPV depressurization, while MELCOR computes a more gradual one. In Fig. 4 which is the comparison of cumulative SRV discharge to suppression pool, it is possible to see the more sharp increase of the cumulative mass in SAMPSON than MELCOR at 7 hours. The observed differences concerning the RPV discharge flow rate are directly connected with hydrogen generation as shown in Fig. 4 and up to the beginning of oxidation phase around 4 hours the calculation results by the two codes are similar. After SAMPSON computes a large amount of hydrogen about 1,600 kg in

1.5 hours against 600 kg in MELCOR in the same timeline . The oxidation is connected with considerable release of energy in the core region, which leads to more quickly heating of the core structures. Therefore the different magnitude of the chemical energy calculated by the two codes can cause certainly different core degradation and melt progression.

5.1.2. RPV Water Level

The RPV water level is maintained for the first hour by the operation of the feedwater and IC systems following SCRAM. After 55 minutes at which the IC operation stops, the water level gradually decreases due to boiling off with steam discharge to the suppression pool by the SRV cycling.
Comparison plot of the swollen water level between SAMPSON and MELCOR is shown in Fig. 5. The initial differences until 2.7 hours are. because the mass of water in MELCOR includes only the water level up to the TAF level [1].
The most remarkable difference in the two simulations is that the core water level in SAMPSON decreases much more quickly than MELCOR especially after hydrogen generation starting around 4 hours. Hydrogen generation causes pressure increase to open the SRV valve, which causes partial evaporation due to depressurization of RPV. SAMPSON produces a total amount of hydrogen generation 2.6 times more than MELCOR so that the water level decreases more quickly than MELCOR. As shown in Fig. 6 which is comparison of SRV mass flow rate, SAMPSON has larger mass flow rate than MELCOR after oxidation starting and this indicates that SAMPSON carries more energy. It should be also mentioned about the SRV mass flow rate comparison that MELCOR simulates less mass flow rate after oxidation starting while SAMPSON has same values before and after except several values thought to be numerical errors. The mass flow rate should decrease after hydrogen generation compared to the case when steam only exists so that this point is remaining issue in SAMPSON.

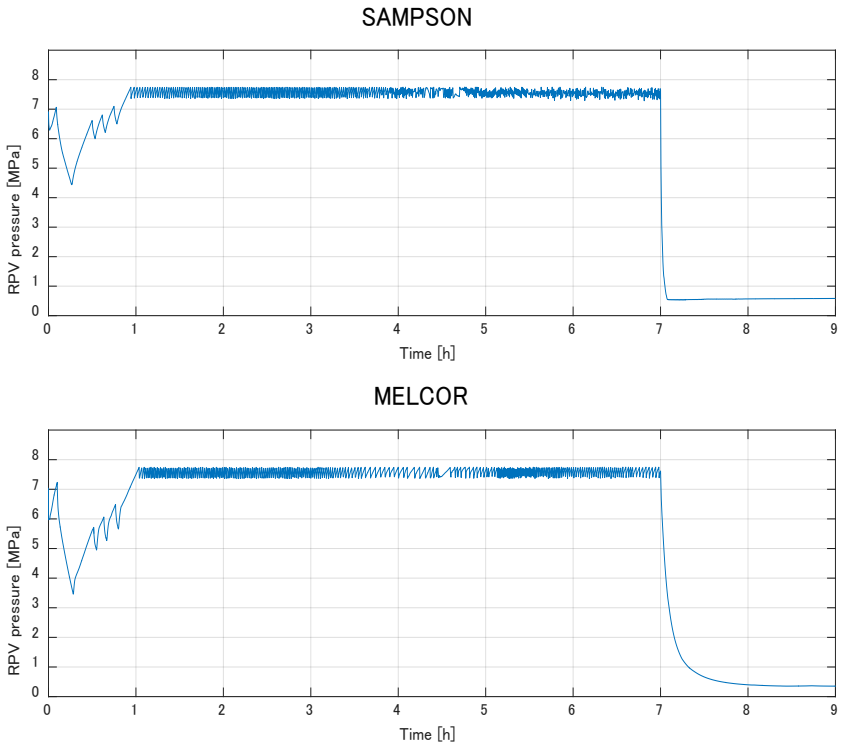

Fig. 3 Comparison of RPV Pressure.

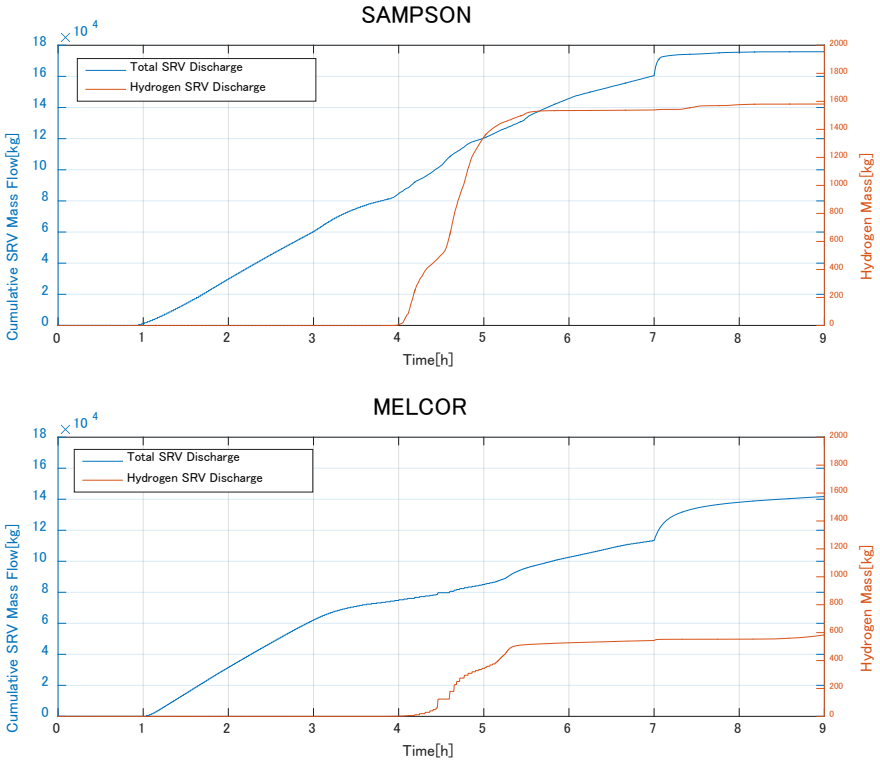

Fig.4 Comparison of Cumulative SRV Discharge to Suppression Pool.

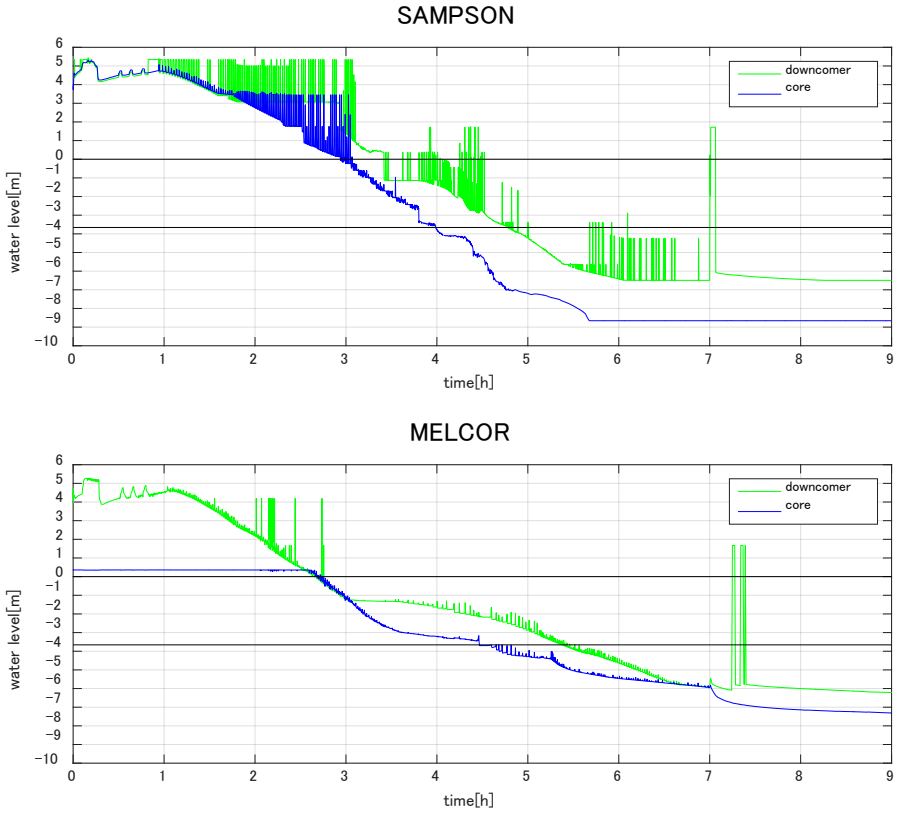

Fig. 5 Comparison of RPV Water Level in Core region and Downcomer.

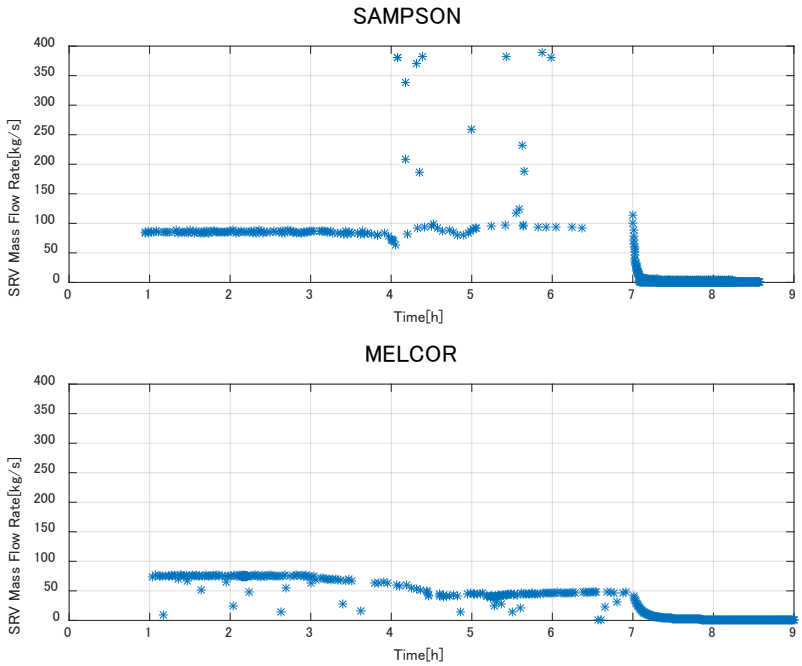

Fig. 6 Comparison of SRV Mass Flow Rate.

5.2 Containment Response

Comparison of the containment pressures with the RPV pressure and hydrogen generation in both of SAMPSON and MELCOR is shown in Fig. 7. The key difference is the amount of hydrogen generation and the containment pressures after 4 hours at which the core degradation starts. Hydrogen mass in SAMPSON is 2.6 times the value computed by MELCOR, which influences directly on the difference in the containment pressures. Hydrogen coming from oxidation of the core materials with steam is discharged by the so that the containment pressures increases due to incondensable hydrogen gases.

5.3 Core Degradation

Comparison of the SAMPSON and MELCOR prediction of the intact fuel temperature in all core nodes is shown in Fig. 8. The temperatures reaching zero indicate that the corresponding node melt and lose their geometries. The SAMPSON simulation shows fuel temperature can increase up to around 3000 K, while the MELCOR ones exhibits about 2500 K. This might be because MELCOR adopts the best practice based on the VERCORS experiments [1] while the current SAMPSON condition is based on the validation result against Phebus FPT-1 [5] and CORA experiments.
It is also the key difference that the SAMPSON fuel temperature increasing rate is sharper compared to MELCOR. The fuel rings reach at 2473 K shortly after oxidation of the Zircaloy cladding starts around 4 hours. It might be caused by that a large amount of the oxidation chemical energy is generated, and accelerates the further oxidation reaction, which leads this steep temperature increasing.
As mentioned in 4.2, both SAMPSON and MELCOR assume that steam can flow through the core debris, which leads increasing of the oxidation surface area. As shown in Fig. 10, the minimum porosity is around 0.4 in SAMPSON while less than 0.2 in MELCOR, this difference of the flow area allowing more contact of steam with the core debris is considered to cause large difference in hydrogen generation.
Another significant different point is that the MELCOR molten debris falls down into the lower plenum while the SAMPSON molten debris remains until the core plate fails as shown in Fig. 9 which is comparison of the SAMPSON and MELCOR debris mass distribution in the core and lower plenum. The MELCOR debris mass gradually increases corresponding to the timings of the fuel failure. The

water level looks like to decrease at the same timing in Fig. 6. The SAMPSON molten debris is kept above the core plate by 7.2 hours because SAMPSON assumes that the debris stop on the plate until temperature of the plate reaches the stainless steel melting point.

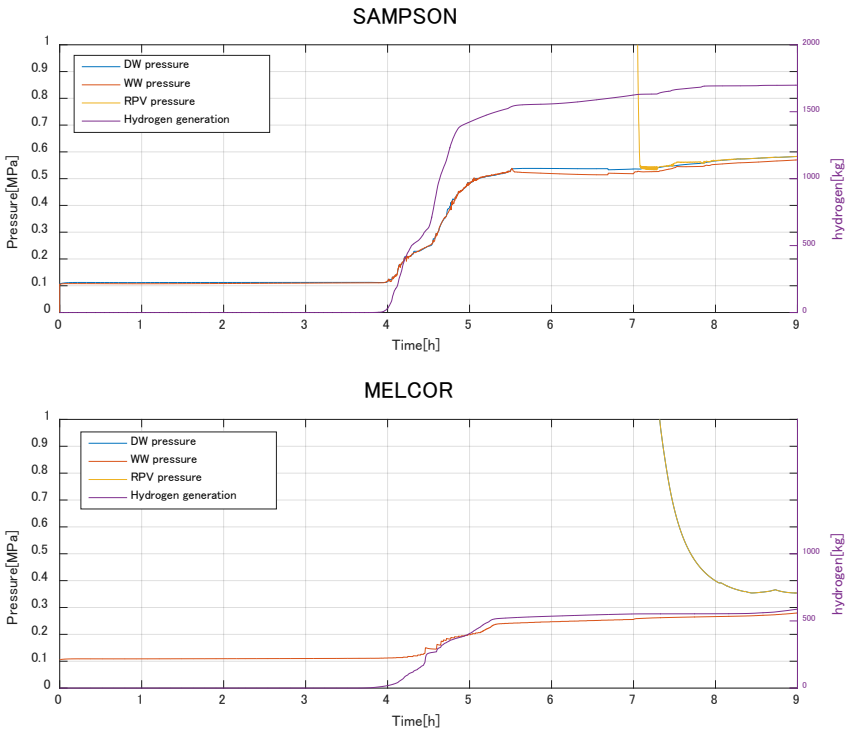

Fig. 7 Comparison of PCV Pressure and Hydrogen generation.

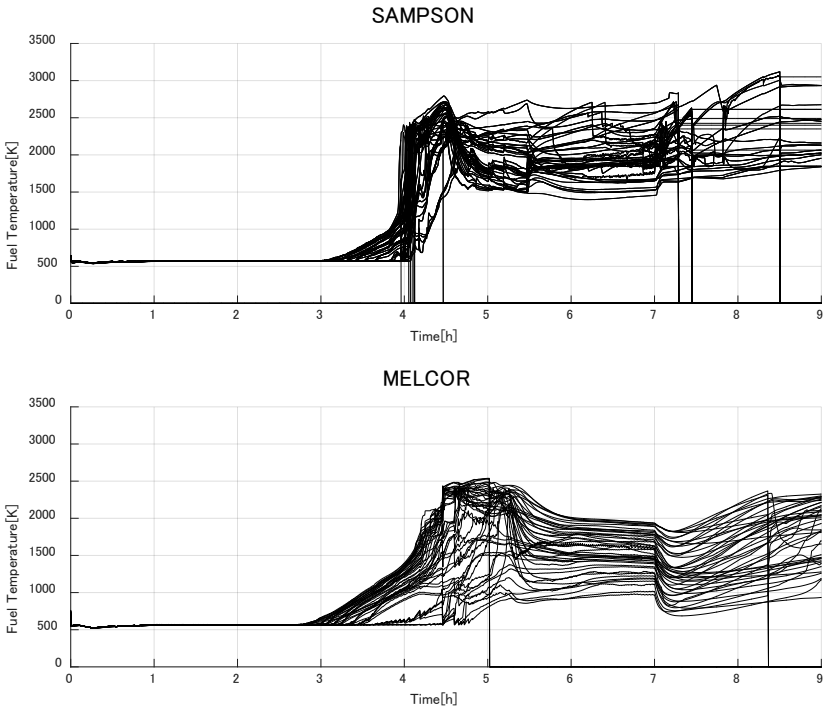

Fig. 8 Comparison of Fuel Temperature.

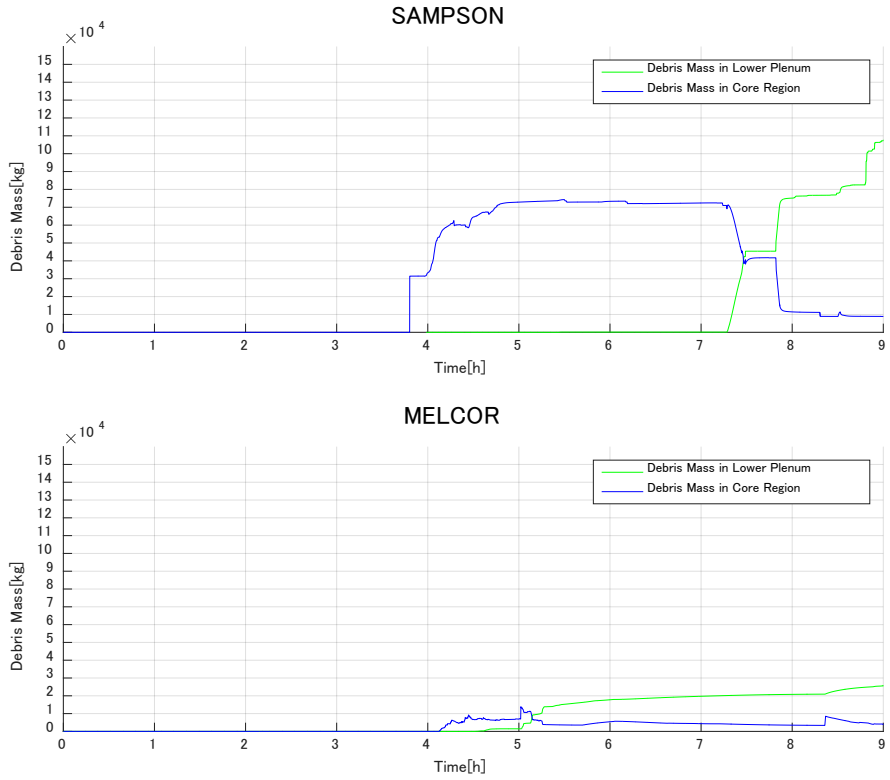

Fig. 9 Comparison of Debris Mass in Core Region and Lower Plenum.

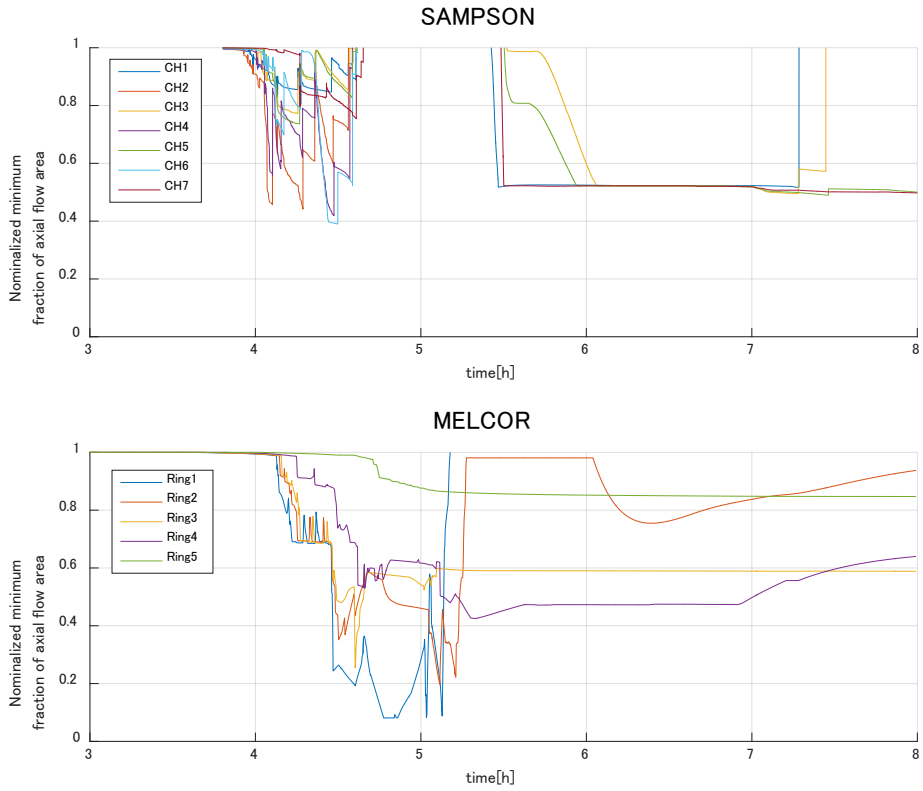

Fig. 10 Comparison of Minimum Vertical Flow Area through the Core Debris.

6. CONCLUSIONS

The SAMPSON simulation against the Fukushima-Daiichi nuclear power station unit 1 with the same condition of the MAAP-MELCOR crosswalk study was performed for 9 hours after SCRAM. The key event timings and some plant parameters of SAMPSON are compared with those of MELCOR reported in the MAAP-MELCOR crosswalk study [1]. The following differences are found:

- ✓ The RPV pressure in SAMPSON shows immediate depressurization after SRV seizure at 7 hours, while MELCOR simulates gradual depressurization.
- ✓ The SAMPSON water levels of the core and downcomer decreases more quickly than those of MELCOR. The water level in the lower head keeps decreasing even though the core debris remains on the core plate due to a large amount of energy carried away through SRV working.
- ✓ SAMPSON computes larger hydrogen generation about 2.6 times of MELCOR . This is related to the steep temperature increase of SAMPSON in which the fuel rods heat up to 2347 K as soon as the oxidation chemical reaction starts, while MELCOR shows more gradual increase. One possibility is the minimum porosity with which steam can flow through the core debris. The SAMPSON minimum porosity is 0.4 while the MELCOR one is about 0.2.

It is challenging to provide complete explanations to these differences, however, since SAMPSON is on the way of development aiming at understanding the Fukushima Daiichi accident phenomena, this comparative study would contribute to the further improvement of severe accident analysis prediction accuracy.

ACKNOWLEDGMENTS

The authors wish to acknowledge to Dr. Gauntt and Dr. Andrews of Sandia National Laboratories for helpful discussion and suggestions.

REFERENCES

1. The Electric Power Research Institute (EPRI), “MAAP-MELCOR Crosswalk: Phase I Study” (2014).
2. The Institute of Applied Enegy (IAE), “Benchmark Study of the Accident at the Fukushima Daiichi Nuclear Power Plant Phase I Final Report” (2015)
3. Sandia National Laboratories (SNL), “MELCOR Computer Code Manuals”, NUREG/CR-6119(2011).
4. A.Costa et al., “Validation of the SAMPSON/MCRA code against CORA-18 experiment”, ICONE-23 (2015).
5. T.Ikeda et al., “Analysis of Core Degradation and Fission Products Release in Phebus FPT1 Test at IRSN by Detailed Severe Accidents Analysis Code, IMPACT/SAMPSON”, GENES4/ANP2003(2003).
6. MATPRO-Version 11 (Revision 2), NUREG/CR-0497(TREE-1280), Rev.2, 1981.